Metals (Ni and Fe) Doped Si, C, BN, AlP Nanotubes and Nanocages as Catalysts for SO_2 Hydro-Desulfurization to Create the H_2S

[1]Xiao Shao*, [2]Farag M. A. Altalbawy, [3]Nawfal Yousif Jamil, [4]Ahmed Salih Sahib
[5]Zahraa Saad Abdulali, [6]Mariem Alwan, [7]Mahmood Jawad, [8]Hiba Mushtaq,
[9]Fadhil F. Sead, [10]Aseel Smerat and [11]Wang Baoo
[1]School of Biological and Pharmaceutical Engineering,
JiLin Agricultural Science and Technology College, JiLin, 132000, China.
[2]Department of Chemistry, University College of Duba, University of Tabuk, Tabuk, Saudi Arabia.
[3]Department of Radiology Techniques, Health and Medical Techniques College,
Alnoor University, Nineveh, Iraq.
[4A]College of pharmacy, Ahl Al Bayt University, Iraq.
[4B]Department of Pharmacology and Toxicology, College of Pharmacy, University of Kerbala, Iraq.
[5]College of Health and Medical Technology, National University of Science and Technology,
Dhi Qar, 64001, Iraq.
[6]Pharmacy college, Al-Farahidi University, Baghdad, Iraq.
[7]Department of Pharmacy, Al-Zahrawi University College, Karbala, Iraq.
[8]Gilgamesh Ahliya University, Baghdad, Iraq.
[9]Department of Chemistry, College of Medical Technology, The Islamic University, Najaf, Iraq.
[10A]Faculty of Educational Sciences, Al-Ahliyya Amman University, Amman 19328, Jordan.
[10B]Department of Biosciences, Saveetha School of Engineering,
Saveetha Institute of Medical and Technical Sciences, Chennai, 602105, India.
[11]Shaoxing Hanli Industrial Automation, Shaoxing, Zhejiang, China.
shaoxiao0325@163.com*

(Received on 8th December 2025, accepted in revised form 6th July 2026)

Suumary: In this work, potential of Ni-Si_{51}, Ni-C_{51}, Fe-C_{71}, Fe-$B_{35}N_{35}$, Ni-$Al_{25}P_{25}$, nanotubes as catalysts for SO_2 hydro-desulfurization are examined to propose the new catalysts with high performances. Results shown that the Ni and Fe adoption on nanocages and nanotubes is improved the catalytic activity of C, Si, BN, AlP nanotubes and nanocages, significantly. The Ni and Fe atoms dues to high adsorption energy values are cites to join the SO_2. Results shown that Ni-Si_{51}, Ni-C_{51}, Fe-C_{71}, Fe-$B_{35}N_{35}$, Ni-$Al_{25}P_{25}$, nanotubes as catalysts for SO_2 hydro-desulfurization have higher catalytic activity than various metals and various metal oxide catalysts. The H_2S is generated on Ni-Si_{51}, Ni-C_{51}, Fe-C_{71}, Fe-$B_{35}N_{35}$, Ni-$Al_{25}P_{25}$, Fe and Ni doped nanotubes: SO_2* → SO* → S* → SH* → H_2S. Finally, Ni-Si_{51}, Fe-$B_{35}N_{35}$, Ni-$Al_{25}P_{25}$, Fe-BNNT and Ni-AlPNT can catalyze the SO_2 hydro-desulfurization.

Keyword: Nanostructure, Metal catalyst, Mechanism, Nanocage, SO_2, H_2S.

Introduction

In recent years, the sulphur in chemical industry through Claus reaction has been produced from SO_2 and H_2S [1, 2]. The researchers in according to environmental laws have been tried to eliminate the sulphur compounds and SO_2 and H_2S as toxic gases [3, 4].

In previous works [7-9] the important of nanotubes and nanocages as effective structures to use as catalysts of various chemical reactions have shown that theses catalysts can be considered as new materials to catalyze the reactions with high efficiency.

The various types of nanocages and nanotubes have high stability and potential to adsorb the species [10-13]. The Ni and Fe metal atoms have suitable electrons in d orbitals for interactions with electrons of p orbitals of Si, C, Al, N, P and B atoms of nanotubes and nanocaes [14-17]. The electrons of p orbitals of S and O in H_2S and SO_2 molecules can interact with suitable electrons in d orbitals for interactions with electrons of p orbitals of Si, C, Al, N, P and B atoms of nanotubes and nanocaes [18-21]. In previous works [22-24] the theoretical methods have been used to examination the catalytic activity of catalysts of important inorganic and organic reactions. The metal doped catalysts have high positions to join the species [25-27].

The potential of metals doped Si, C, BN, AlP nanocages and nanotubes **(**Ni-Si_{51}, Ni-C_{51}, Fe-C_{71}, Fe-$B_{35}N_{35}$, Ni-$Al_{25}P_{25}$) for SO_2 hydro-desulfurization are examined. The pathways for SO_2 hydro-desulfurization to produce the H_2S on Ni-Si_{51}, Ni-C_{51}, Fe-C_{71}, Fe-$B_{35}N_{35}$,

***To whom all correspondence should be addressed.**

$Ni\text{-}Al_{25}P_{25}$, Fe and Ni doped nanotubes are investigated. The abilities of $Ni\text{-}Si_{51}$, $Ni\text{-}C_{51}$, $Fe\text{-}C_{71}$, $Fe\text{-}B_{35}N_{35}$, $Ni\text{-}Al_{25}P_{25}$, Fe and Ni doped nanotubes to produce the H_2S are compared with metal catalysts [13-18].

In this work, we have compared the catalytic potential of $Ni\text{-}Si_{51}$, $Ni\text{-}C_{51}$, $Fe\text{-}C_{71}$, $Fe\text{-}B_{35}N_{35}$, $Ni\text{-}Al_{25}P_{25}$, Fe and Ni doped nanotubes for SO_2 hydro-desulfurization to H_2S production. Here, we have tried to propose the mechanisms for SO_2 hydro-desulfurization on $Ni\text{-}Si_{51}$, $Ni\text{-}C_{51}$, $Fe\text{-}C_{71}$, $Fe\text{-}B_{35}N_{35}$, $Ni\text{-}Al_{25}P_{25}$, Fe and Ni doped nanotubes. Here, we have tried to compare the efficiency of $Ni\text{-}Si_{51}$, $Ni\text{-}C_{51}$, $Fe\text{-}C_{71}$, $Fe\text{-}B_{35}N_{35}$, $Ni\text{-}Al_{25}P_{25}$ with other catalysts.

Computational details

The geometries of $Ni\text{-}Si_{51}$, $Ni\text{-}C_{51}$, $Fe\text{-}C_{71}$, $Fe\text{-}B_{35}N_{35}$, $Ni\text{-}Al_{25}P_{25}$, and interactions with species have been optimized by M06-2X/cc-pVQZ model in GAMESS software [22-25]. In this study, the force set is 1.4×10^{-5} Hartree/Bohr and displacement is 4.0×10^{-6} Å, the 48 k-points and 0.0054 eV are cutoff energy, RMS force is 0.000036 and the RMS displacement is 0.000072 for optimizing the $Ni\text{-}Si_{51}$, $Ni\text{-}C_{51}$, $Fe\text{-}C_{71}$, $Fe\text{-}B_{35}N_{35}$, $Ni\text{-}Al_{25}P_{25}$, and interactions with species [23-25]. In this study, BSSE to calculate the interaction energy between the $Ni\text{-}Si_{51}$, $Ni\text{-}C_{51}$, $Fe\text{-}C_{71}$, $Fe\text{-}B_{35}N_{35}$, $Ni\text{-}Al_{25}P_{25}$, and interactions with species have been calculated by counterpoise method (CP) [25].

The adsorption energy ($\Delta E_{adsorption}$) of species on $Ni\text{-}Si_{51}$, $Ni\text{-}C_{51}$, $Fe\text{-}C_{71}$, $Fe\text{-}B_{35}N_{35}$, $Ni\text{-}Al_{25}P_{25}$, Fe and Ni doped nanotubes are examined [28, 29]:

$$\Delta E_{adsorption} = E_{nano\text{-}specie} - E_{nano} - E_{specie} \quad (1)$$

The $E_{nano\text{-}specie}$ is energy of catalysts-species, E_{nano} is energy of catalysts and E_{specie} is energy of species [30, 31]. The $E_{activation}$ and $\Delta G_{reaction}$ of SO_2 hydro-desulfurization are examined [32, 33]:

$$E_{activation} = E_{transition\ state} - E_{reactant} \quad (2)$$

$$\Delta G_{reaction} = G_{product} - G_{reactant} \quad (3)$$

The adoption energy ($\Delta E_{adoption}$) of Fe and Ni atoms on catalysts are examined [34-37]:

$$\Delta E_{adoption} = E_{nano\text{-}metal} - E_{nano} - E_{metal} \quad (4)$$

The formation energy ($\Delta E_{formation}$) of catalysts are examined [38-40]:

$$\Delta E_{formation} = E_{nano\text{-}metal} - n * E_X - E_{metal} \quad (5)$$

The $E_{nano\text{-}metal}$ is energy of $Ni\text{-}Si_{51}$, $Ni\text{-}C_{51}$, $Fe\text{-}C_{71}$, $Fe\text{-}B_{35}N_{35}$, $Ni\text{-}Al_{25}P_{25}$, Fe and Ni doped nanotubes [40].

Results and discussion

Adsorption of species on $Ni\text{-}Si_{51}$, $Ni\text{-}C_{51}$, $Fe\text{-}C_{71}$, $Fe\text{-}B_{35}N_{35}$, $Ni\text{-}Al_{25}P_{25}$, nanotubes

The potential of $Ni\text{-}Si_{51}$, $Ni\text{-}C_{51}$, $Fe\text{-}C_{71}$, $Fe\text{-}B_{35}N_{35}$, $Ni\text{-}Al_{25}P_{25}$, Fe and Ni doped nanotubes catalysts to join the species are examined. In Fig 1 and Fig 2, the structures of $Ni\text{-}Si_{51}$, $Ni\text{-}C_{51}$, $Fe\text{-}C_{71}$, $Fe\text{-}B_{35}N_{35}$, $Ni\text{-}Al_{25}P_{25}$, nanotubes are shown. The $\Delta E_{formation}$ of $Ni\text{-}Si_{51}$, $Ni\text{-}C_{51}$, $Fe\text{-}C_{71}$, $Fe\text{-}B_{35}N_{35}$, $Ni\text{-}Al_{25}P_{25}$, nanotubes in gas phase and water as polar solvent are reported in Table 1. The $\Delta E_{adoption}$ of $Ni\text{-}Si_{51}$, $Ni\text{-}C_{51}$, $Fe\text{-}C_{71}$, $Fe\text{-}B_{35}N_{35}$, $Ni\text{-}Al_{25}P_{25}$, Fe and Ni doped nanotubes in gas phase and water as polar solvent are reported in Table-1.

The $\Delta E_{adoption}$ of $Ni\text{-}Si_{51}$, $Ni\text{-}C_{51}$, $Fe\text{-}C_{71}$, $Fe\text{-}B_{35}N_{35}$, $Ni\text{-}Al_{25}P_{25}$, Fe and Ni doped nanotubes are negative and so the Fe and Ni adoption can increase the stability of $Ni\text{-}Si_{51}$, $Ni\text{-}C_{51}$, $Fe\text{-}C_{71}$, $Fe\text{-}B_{35}N_{35}$, $Ni\text{-}Al_{25}P_{25}$. The Fe and Ni of $Ni\text{-}Si_{51}$, $Ni\text{-}C_{51}$, $Fe\text{-}C_{71}$, $Fe\text{-}B_{35}N_{35}$, $Ni\text{-}Al_{25}P_{25}$ are catalytic positions to join the SO_2 hydro-desulfurization species. The $\Delta E_{adoption}$ of $Ni\text{-}Si_{51}$, $Fe\text{-}B_{35}N_{35}$, $Ni\text{-}Al_{25}P_{25}$, Fe-BNNT are more negative than $Ni\text{-}C_{51}$, $Fe\text{-}C_{71}$, Ni-CNT and Fe-CNT. The $\Delta E_{formation}$ of $Ni\text{-}Si_{51}$, $Ni\text{-}C_{51}$, $Fe\text{-}C_{71}$, $Fe\text{-}B_{35}N_{35}$, $Ni\text{-}Al_{25}P_{25}$, Fe and Ni doped nanotubes are negative. The $E_{formation}$ of Fe-CNT, Ni-CNT, Fe-BNNT and Ni-AlPNT are higher than $Ni\text{-}C_{51}$, $Ni\text{-}Al_{25}P_{25}$, $Ni\text{-}Si_{51}$, $Fe\text{-}C_{71}$, $Fe\text{-}B_{35}N_{35}$. The $E_{formation}$ of $Ni\text{-}Al_{25}P_{25}$, $Ni\text{-}Si_{51}$, $Fe\text{-}B_{35}N_{35}$ are higher than $Fe\text{-}C_{71}$, $Ni\text{-}C_{51}$.

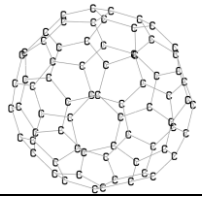	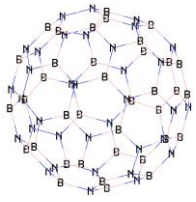	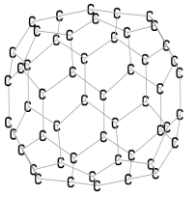	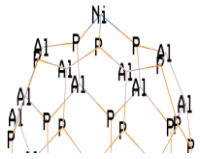
C_{71}	**$B_{35}N_{35}$**	**C_{51}**	**$Ni\text{-}Al_{25}P_{25}$**

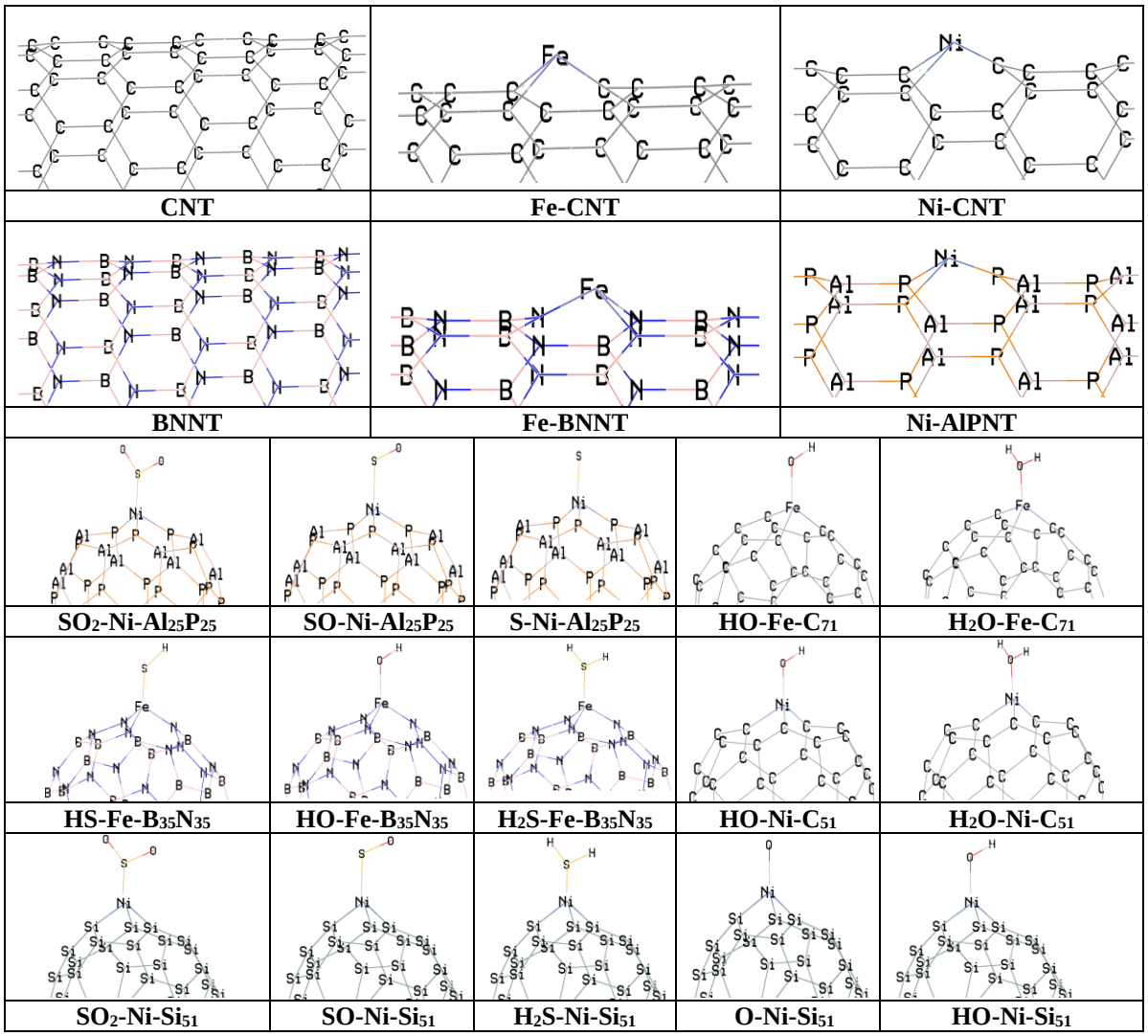

Fig. 1: The catalysts and interactions with SO_2 hydro-desulfurization species.

Table-1: The $\Delta E_{foramtion}$ and $\Delta E_{adoption}$ of in eV and $\Delta E_{adsorption}$ of important species in eV.

Nanostructure	$\Delta E_{formation}$	$\Delta E_{adoption}$	Nanostructure	$\Delta E_{formation}$	$\Delta E_{adoption}$
Ni-C_{51}	-3.72	-3.77	Fe-C_{71}	-3.52	-3.63
Ni-$Al_{25}P_{25}$	-4.01	-4.14	Fe-$B_{35}N_{35}$	-3.87	-3.92
Ni-CNT	-4.74	-4.85	Fe-CNT	-4.52	-4.61
Ni-AlPNT	-5.23	-5.33	Fe-BNNT	-4.94	-5.12
Ni-Si_{51}	-4.95	-5.11	Ni-Si_{51}	-4.95	-5.13

$\Delta E_{adsorption}$ in gas phase

Species	Ni-C_{51}	Ni-$Al_{25}P_{25}$	Ni-CNT	Fe-$B_{35}N_{35}$	Fe-CNT	Fe-BNNT
SO_2	-4.04	-4.13	-4.34	-3.94	-4.13	-4.33
SO	-3.45	-3.54	-3.73	-3.38	-3.52	-3.72
S	-2.42	-2.51	-2.62	-2.40	-2.51	-2.64
O	-2.76	-2.84	-3.01	-2.72	-2.87	-3.01
SH	-0.14	-0.15	-0.17	-0.13	-0.14	-0.16
OH	-0.07	-0.07	-0.05	-0.07	-0.06	-0.07
H_2S	-0.21	-0.24	-0.24	-0.23	-0.23	-0.25
H_2O	-0.08	-0.11	-0.13	-0.11	-0.15	-0.12

$\Delta E_{adsorption}$ [13-18]	SO_2	SO	S	O	SH	OH	H_2S	H_2O
Various metal catalysts [13-15]	-3.37	-2.84	-2.02	-2.33	-0.13	-0.08	-0.15	-0.09
Various metal oxide catalysts [16-18]	-3.42	-2.93	-2.14	-2.37	-0.10	-0.06	-0.18	-0.07

The $\Delta E_{adsorption}$ of species on catalysts in gas phase and water as polar solvent are investigated in Table 1. The complexes of Ni-Si_{51}, Ni-C_{51}, Fe-C_{71}, Fe-$B_{35}N_{35}$, Ni-$Al_{25}P_{25}$, Fe and Ni doped nanotubes with species for SO_2 hydro-desulfurization are presented in Figs 2 and 3. In this work, we reported the published data [13-18] for examination of potential of various metal catalysts and various metal oxide catalysts for SO_2 hydro-desulfurization to H_2S production in Tables 2 and 3 and we compared the obtained results in this work with published data in previous works about emanation of potential of various metal catalysts and various metal oxide catalysts for SO_2 hydro-desulfurization to H_2S production. The Ni-Si_{51}, Ni-C_{51}, Fe-C_{71}, Fe-$B_{35}N_{35}$, Ni-$Al_{25}P_{25}$ for SO_2 hydro-desulfurization have higher potential to adsorb the species than various metals and various metal oxide catalysts.

In previous works [7-9] the important of nanotubes and nanocages as effective structures to use as catalysts of various chemical reactions have been examined and catalysts can be considered as new materials to catalyze the reactions with high efficiency in normal temperature. In previous works [22-24] the theoretical methods have been used to examination the catalytic activity of catalysts of important inorganic and organic reactions. The metal catalysts have effective positions adsorb the species by theoretical models [25-27].

It can be concluded that the H_2O and H_2S as final production for SO_2 hydro-desulfurization are desorbed from Ni-Si_{51}, Ni-C_{51}, Fe-C_{71}, Fe-$B_{35}N_{35}$, Ni-$Al_{25}P_{25}$, easily. The S specie is joined on Fe and Ni of Ni-Si_{51}, Ni-C_{51}, Fe-C_{71}, Fe-$B_{35}N_{35}$, Ni-$Al_{25}P_{25}$, Fe and Ni doped nanotubes with the higher $\Delta E_{adsorption}$ than other species.

SO_2 hydro-desulfurization on Ni-Si_{51}, Ni-C_{51}, Fe-C_{71}, Fe-$B_{35}N_{35}$, Ni-$Al_{25}P_{25}$

The pathways of SO_2 hydro-desulfurization on Ni-Si_{51}, Ni-C_{51}, Fe-C_{71}, Fe-$B_{35}N_{35}$, Ni-$Al_{25}P_{25}$, Fe and Ni doped nanotubes are examined. The $E_{activation}$ and $\Delta G_{reaction}$ of SO_2 hydro-desulfurization on Ni-Si_{51}, Ni-C_{51}, Fe-C_{71}, Fe-$B_{35}N_{35}$, Ni-$Al_{25}P_{25}$ are presented in Table 2. In Figs 2 and 3, the structures of SO_2 hydro-desulfurization species on Ni-Si_{51}, Ni-C_{51}, Fe-C_{71}, Fe-$B_{35}N_{35}$, Ni-$Al_{25}P_{25}$ are shown.

In this work, we reported the published data [13-18] for examination of potential of various metal catalysts and various metal oxide catalysts for SO_2 hydro-desulfurization to H_2S production in Tables 2 and 3 and we compared the obtained results in this work with published data in previous works about emanation of potential of various metal catalysts and various metal oxide catalysts for SO_2 hydro-desulfurization to H_2S production. The Ni-Si_{51}, Ni-C_{51}, Fe-C_{71}, Fe-$B_{35}N_{35}$, Ni-$Al_{25}P_{25}$ for SO_2 hydro-desulfurization have higher catalytic activity than various metals and various metal oxide catalysts.

The adsorbed SO_2 on Ni-Si_{51}, Ni-C_{51}, Fe-C_{71}, Fe-$B_{35}N_{35}$, Ni-$Al_{25}P_{25}$, Fe and Ni doped nanotubes is dissociated: Metal-SO_2 → Metal-SO* + Metal-O* and the Metal-SO* + Metal-S*. Results shown that these reaction steps (Metal-SO_2 → Metal-SO*→ Metal-S*) are possible from thermodynamic view points on Ni-Si_{51}, Ni-C_{51}, Fe-C_{71}, Fe-$B_{35}N_{35}$, Ni-$Al_{25}P_{25}$.

The Ni-Si_{51}, Ni-C_{51}, Fe-C_{71}, Fe-$B_{35}N_{35}$, Ni-$Al_{25}P_{25}$ for SO_2 hydro-desulfurization have higher catalytic activity than various metals and various metal oxide catalysts. The Ni-Si_{51}, Ni-C_{51}, Fe-C_{71}, Fe-$B_{35}N_{35}$, Ni-$Al_{25}P_{25}$ for SO_2 hydro-desulfurization have higher potential to adsorb the species than various metals and various metal oxide catalysts.

The dissociation of H_2 on Ni-Si_{51}, Ni-C_{51}, Fe-C_{71}, Fe-$B_{35}N_{35}$, Ni-$Al_{25}P_{25}$, Fe and Ni doped nanotubes has low $E_{activation}$. The dissociation of SO_2 and H_2 molecules on Ni-Si_{51}, Ni-C_{51}, Fe-C_{71}, Fe-$B_{35}N_{35}$, Ni-$Al_{25}P_{25}$, Fe and Ni doped nanotubes are spontaneous reactions. The $\Delta G_{reaction}$ values of Fe-$B_{35}N_{35}$ and Fe-BNNT are higher than Fe-C_{71} and Fe-CNT.

The $\Delta G_{reaction}$ of Metal-SO* + Metal-S* reaction on Ni-Si_{51}, Ni-C_{51}, Fe-C_{71}, Fe-$B_{35}N_{35}$, Ni-$Al_{25}P_{25}$, Fe and Ni doped nanotubes has more negative than Metal-SO_2 → Metal-SO* + Metal-O* reaction. The $E_{activation}$ of Metal-SO* + Metal-S* on Ni-Si_{51}, Ni-C_{51}, Fe-C_{71}, Fe-$B_{35}N_{35}$, Ni-$Al_{25}P_{25}$, Fe and Ni doped nanotubes surfaces are lower than Metal-SO_2 → Metal-SO* + Metal-O* reaction. The Fe doped nanotubes have higher $\Delta G_{reaction}$ than Fe-C_{71} and Fe-$B_{35}N_{35}$.

In other pathway on Ni-Si_{51}, Ni-C_{51}, Fe-C_{71}, Fe-$B_{35}N_{35}$, Ni-$Al_{25}P_{25}$, Fe and Ni doped nanotubes: Metal-O* → Metal-OH* → Metal* + H_2O and H_2O is produced. The Metal-O* → Metal-OH* has negative $\Delta G_{reaction}$ and Metal-OH* → Metal* + H_2O has positive $\Delta G_{reaction}$ on Ni-Si_{51}, Ni-C_{51}, Fe-C_{71}, Fe-$B_{35}N_{35}$, Ni-$Al_{25}P_{25}$, Fe and Ni doped nanotubes surfaces. The Metal-O* → Metal-OH* → Metal* + H_2O due to $E_{activation}$ and $\Delta G_{reaction}$ cannot be processed on Ni-Si_{51}, Ni-C_{51}, Fe-C_{71}, Fe-$B_{35}N_{35}$, Ni-$Al_{25}P_{25}$, Fe and Ni doped nanotubes. The H_2S is desorbed from Ni-Si_{51}, Ni-C_{51}, Fe-C_{71}, Fe-$B_{35}N_{35}$, Ni-$Al_{25}P_{25}$, Fe and Ni doped nanotubes. The Ni-Si_{51}, Fe-$B_{35}N_{35}$, Fe-BNNT and Ni-AlPNT can catalyze the SO_2 hydro-desulfurization from thermodynamic view point.

Table-2: The $E_{activation}$ and $\Delta G_{reaction}$ of reaction steps for SO_2 hydro-desulfurization in eV.

$E_{activation}$ and $\Delta G_{reaction}$ in gas phase						
Nano-catalysts	**Ni-C_{51}**		**Ni-$Al_{25}P_{25}$**		**Ni-Si_{51}**	
SO_2 hydro-desulfurization	**$E_{activation}$**	**$\Delta G_{reaction}$**	**$E_{activation}$**	**$\Delta G_{reaction}$**	**$E_{activation}$**	**$\Delta G_{reaction}$**
$SO_2 \rightarrow SO^*$	**0.32**	**-0.44**	**0.31**	**-0.46**	**0.28**	**-0.51**
$SO^* \rightarrow S^*$	**0.63**	**-1.33**	**0.60**	**-1.39**	**0.56**	**-1.53**
$H_2 \rightarrow H^*$	**0.01**	**-0.60**	**0.01**	**-0.57**	**0.01**	**-0.53**
$S^* \rightarrow SH^*$	**1.18**	**0.83**	**1.11**	**0.79**	**1.03**	**0.73**
$SH^* \rightarrow H_2S$	**1.42**	**-0.28**	**1.34**	**-0.29**	**1.24**	**-0.32**
$O^* \rightarrow OH^*$	**1.10**	**-0.13**	**1.04**	**-0.13**	**0.96**	**-0.15**
$OH^* \rightarrow H_2O$	**3.21**	**-0.98**	**3.04**	**-1.03**	**2.81**	**-1.13**
Nano-catalysts	**Fe-C_{71}**		**Fe-CNT**		**Fe-BNNT**	
SO_2 hydro-desulfurization	**$E_{activation}$**	**$\Delta G_{reaction}$**	**$E_{activation}$**	**$\Delta G_{reaction}$**	**$E_{activation}$**	**$\Delta G_{reaction}$**
$SO_2 \rightarrow SO^*$	**0.31**	**-0.42**	**0.28**	**-0.47**	**0.25**	**-0.51**
$SO^* \rightarrow S^*$	**0.60**	**-1.25**	**0.54**	**-1.38**	**0.51**	**-1.51**
$H_2 \rightarrow 2\ H^*$	**0.01**	**-0.57**	**0.01**	**-0.51**	**0.01**	**-0.48**
$S^* \rightarrow SH^*$	**1.12**	**0.79**	**1.01**	**0.71**	**0.95**	**0.66**
$SH^* \rightarrow H_2S$	**1.35**	**-0.25**	**1.21**	**-0.29**	**1.15**	**-0.32**
$O^* \rightarrow OH^*$	**1.04**	**-0.12**	**0.94**	**-0.13**	**0.89**	**-0.15**
$OH^* \rightarrow H_2O$	**3.06**	**-0.93**	**2.74**	**-1.02**	**2.60**	**-1.12**
$\Delta G_{reaction}$ [13-18]		**$SO_2 \rightarrow SO^*$**	**$SO^* \rightarrow S^*$**	**$H_2 \rightarrow H^*$**	**$O^* \rightarrow OH^*$**	**$OH^* \rightarrow H_2O$**
Various metal catalysts [13-15]		**-0.34**	**-1.11**	**0.52**	**-0.12**	**-0.80**
Various metal oxide catalysts [16-18]		**-0.37**	**-1.14**	**0.53**	**-0.10**	**-0.85**
$G_{activation}$ [13-18]		**$SO_2 \rightarrow SO^*$**	**$SO^* \rightarrow S^*$**	**$H_2 \rightarrow H^*$**	**$O^* \rightarrow OH^*$**	**$OH^* \rightarrow H_2O$**
Various metal catalysts [13-15]		**0.32**	**0.65**	**0.03**	**1.11**	**3.20**
Various metal oxide catalysts [16-18]		**0.34**	**0.61**	**0.02**	**1.06**	**3.15**

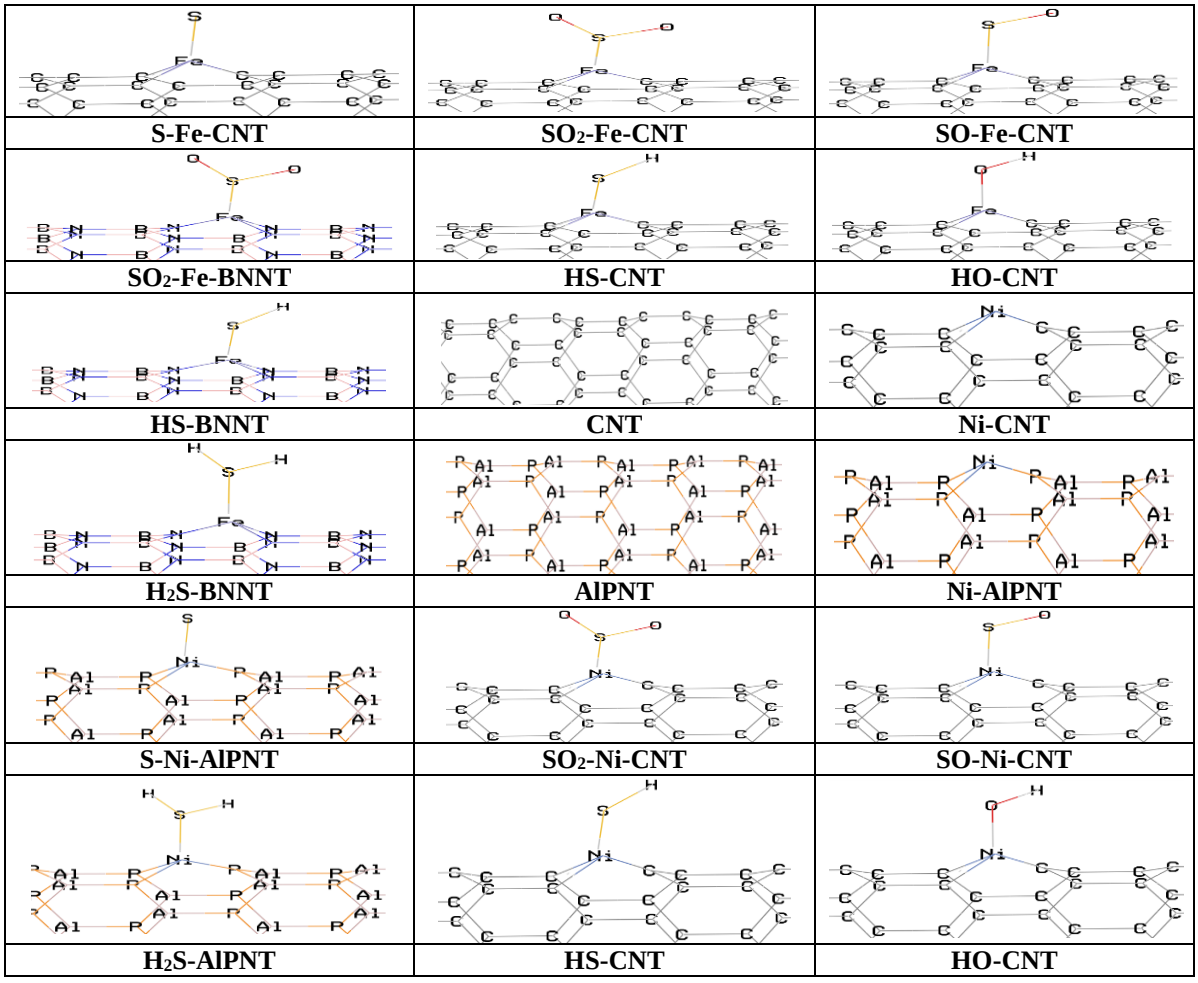

Fig. 2: The interactions of catalysts with SO_2 hydro-desulfurization species.

Conclusion

In this study, the Ni and Fe adoption on nanocages and nanotubes is improved the catalytic activity of C, Si, BN, AlP nanotubes and nanocages, significantly. The $E_{formation}$ of Ni-C_{51}, Ni-$Al_{25}P_{25}$, Ni-CNT, Ni-Si_{51}, Fe-C_{71}, Fe-$B_{35}N_{35}$, Fe-CNT, Fe-BNNT and Ni-AlPNT are -3.70, -4.03, -4.75, -5.22, -4.98, -3.53, -3.84, -4.53 and -4.98 eV. The Ni and Fe atoms dues to high adsorption energy values are cities to join to SO_2. The adsorbed SO_2 on Fe doped nanostructures is dissociated: Metal-SO_2 → Metal-SO* → Metal-S*. The H_2S is generated on Fe and Ni doped Ni-Si_{51}, Ni-C_{51}, Fe-C_{71}, Fe-$B_{35}N_{35}$, Ni-$Al_{25}P_{25}$, Fe and Ni doped nanotubes through these reactions: Metal-S* → Metal-SH* → Metal* + H_2S. The Ni-Si_{51}, Ni-C_{51}, Fe-C_{71}, Fe-$B_{35}N_{35}$, Ni-$Al_{25}P_{25}$, nanotubes as catalysts for SO_2 hydro-desulfurization have higher catalytic activity than various metals and various metal oxide catalysts. The H_2S is released as following: Metal-SO_2* → Metal-SO* → Metal-S* → Metal-SH* → Metal* + H_2S. The Ni-Si_{51}, Fe-$B_{35}N_{35}$, Ni-$Al_{25}P_{25}$, Fe-BNNT and Ni-AlPNT can catalyze the SO_2 hydro-desulfurization.

Acknowledgement

We thank our university for their computational support.

References

1. L. Yue-Qun, T. Xiao-Mao, A chemopalette strategy for white light by modulating monomeric, *Inorg. Chem.* **62**, 12099 (2023).
2. X. Xiao-Hong, W. Zhang-Wen, Creating Optimal Pockets in a Clathrochelate-Based Metal–Organic, *J. Am. Chem. Soc.*, **145**, 14354 (2023).
3. F. Zohreh, C. Hossein. Self-Assembly of Modular Bis-MPA Dendrons into Colloidal Particles, *ACS Omega*, **8**, 252 (2023).
4. M. Aileen, K. Michael, Fabrication of Multifunctional Electronic Textiles Using Oxidative, *J. Am. Chem. Soc.*, **144**, 23297 (2022).
5. G. D. Samuel, K. G. Nishesh, Mn-CUK-1: A Flexible MOF for SO2, H2O, and H2S Capture, *Inorg. Chem.*, **61**, 15037 (2022).
6. A. J. Richard, Z. Chen, Heteroatom-Doped Porous Carbons as Effective Adsorbers for Toxic, *ACS Appl. Mater. Interfaces*, **14**, 33173 (2022).
7. A. U. Rahman, D. M. Saaduzzaman, S. M. Hasan, Aluminum-derived nanotubes for lung cancer detection: a DFT, *Sci. Rep.*, **15**, 34852 (2025).
8. A. U. Rahman, M. Amin, D. M. Saaduzzaman, S. M. Hasan, Early Diagnosis of Tuberculosis by Analyzing the Breath of Patients, *J. Nanotechn*., **1**, 9487892 (2025).
9. S.M. Hasan, M. K. U. Sikder, Designing nitride-derived fullerenes X20N20 (X = B, Al, and Ga) for H2S, *Nanoscale*, **17**, 24755 (2025).
10. A. Beheshti, M. Bahrani-Pour, Photo-Responsive Brominated Hydrogen-Bonded Liquid Crystals, *Crystal Growth Design*, **22**, 4343 (2022).
11. H. Wang, P. Wu, C. Li, Rapid, selectivity, and reversibility absorption of SO 2 via purine, *ACS Sustainable Chem. Eng.*, **10**, 4451 (2022).
12. Z. Geng, S. Ma, Y. Li, Sigmoid Correlations for Gas Solubility and Enthalpy Change for H2S and SO2, *Industrial Eng. Chem. Res.*, **61**, 4493 (2022).
13. F. M. A. Altalbawy, B. M. Yaseen, A. F. Al-Hussainy, SO2 Hydro-Desulfurization to H2S Production Through the Cu-C84, *Silicon*, 17, **563** (2025).
14. P. Brandt, S. Xing, Zirconium and Aluminum MOFs for Low-Pressure SO2 Adsorption, *ACS Appl. Mater. Interfaces*, **13**, 29137 (2021).
15. J. Feng, F. Wang, Cu/HZSM-5 Sorbent Treated by NH3 Plasma for Low-Temperature, *ACS Appl. Mater. Interfaces*, **13**, 24670 (2021).
16. S. Valencia-Loza, Adsorption Mechanism and Regeneration Performance of 13X, *ACS Appl. Mater. Interfaces*, **13**, 18658 (2021).
17. X. Xu, Selective adsorption of sulphur dioxide and hydrogen sulphide by nano catalysts, *Energy Fuels*, **35**, 5110 (2021).
18. X. Wang, F. Yao, Improved conductivity in tape casted Li-NASICON supported thick films, *Nano Lett.*, **21**, 1679 (2021).
19. F. Feng, K. Li, nanocages by NH3 Plasma for SO2 to H2S, *ACS Appl. Mat. Interfaces*, **15**, 2465 (2024).
20. S. Valencia-Loza, Spinel integrated layered oxide cathodes for sodium-ion batteries, *ACS Appl. Mater. Interfaces*, **24**, 4353 (2023).
21. X. Xu, P. Wu, C. Li, Reversible Removal of SO2 with Amine-Functionalized ZIF8, *Energy Fuels*, **35**, 5110 (2021).
22. M. J. Saadh, M. A. Mustafa, K. M. Batoo, Performances of nanotubes and nanocages as anodes in Na-ion, *Ionics*, **30**, 2657 (2024).
23. K. M. Batoo, H. H. Ahmed, M. A. Al-Maliky, Theoretical Investigation of Drug Delivery of Cimetidine as Drug of Coronavirus Disease by Silicon Nanotubes and Silicon Nanocages, *Silicon*, **16**, 2349 (2024).
24. D. Singh, H. Ahmad, Y. A. Naeem, Silicon, Carbon, Germanium, Aluminum Nitride nanocages (Si60, C60, Ge60, Al30N30) as catalysts of N2 reduction to NH3, *Silicon*, **16**, 3011 (2024).

25. A. D. J. A. Bayati, F. Al-dolaimy, K. M. Batoo, A novel two-dimensional monolayer tetragonal boron carbide as a promising anode for Mg-ion, *J. Mol. Model.* **29**, 272 (**2023**).
26. M. J. Saadh, M. A. Mustafa, Q. H. Aziz, Metal Doped Nanocages and Metal Doped Nanotubes as Effective Catalysts for ORR and OER, *Silicon*, **16**, 5739 (2024).
27. E. Naranjo, B. Abd Alreda, M. Zaidi, K. M. Batoo, Nanocages and nanotubes as catalysts for ORR and OER processes, *J. Phys. Chem. Solids*, **187**, 111856 (2025).
28. J. Yao, C. Li, K. Sun, Y. Cai, H. Li, W. Ouyang, H. Li, Ndc-scene: Boost monocular 3d semantic scene completion in normalized device coordinates space. *IEEE/CVF Int. Computer Vision* **11**, 9455 (2023).
29. P. Li, J. Abbas, D. Balsalobre-Lorente, Q. Wang, Q. Zhang, S. A. R. Shah, Impact of sectoral mix on environmental sustainability: How is heterogeneity addressed? *Gondwana Res.* **128**, 86 (2024).
30. J. X. Chen, L. Peng, J. Ma, H. P. Ying, Liberation of a pinned spiral wave by a rotating electric pulse. *Euro. phys. Lett.*, **107**, 38001 (2014).
31. X. Sun, S. Zhu, J. Guo, S. Peng, X. Qie, Z. Yu, P. Li, exploring ways to improve China's ecological well-being amidst air pollution challenges using mixed methods. *J. Environ. Management*, **364**, 121457 (2024).
32. M. Wang, W. Xu, H. Xu, H. Mu, J. Mi, Y. Wu, B. Cai, Evaluation of mechanical properties and geological features of highly sandy dolomite: consequences for engineering safety. *Bulletin Eng. Geology Environ.,* **84**, 603 (2025).
33. S. Jiang, J. Zhang, K. Diao, X. Liu, Z. Ding, Research Advances in Solvent Extraction of Lithium: The Potential of Ionic Liquids. *Adv. Functional Mat.*, **11**, 2423566 (2025).
34. X. Sun, Z. Meng, X. Zhang, J. Wu, The role of institutional quality in the nexus between green financing and sustainable development. *Res. Int. Business Finance*, **73**, 102531 (2025).
35. M. M. Khotbehsara, M. Zadshir, B. M. Miyandehi, E. Mohseni, S. Rahmannia, S. Fathi, Rheological, mechanical and durability properties of self-compacting mortar containing nano-TiO2 and fly ash. *J. American Sci.*, **10**, 222 (2014).
36. B. Mehdizadeh, K. Vessalas, B. Ben, A. Castel, S. Deilami, H. Asadi, Advances in Characterization of Carbonation Behavior in Slag-Based Concrete Using Nanotomography. *Int. Variability*, **1**, 297 (2022).
37. B. Mehdizadeh, K. Vessalas, A. Castel, M. Mortazavi, Investigation of Carbonation Behaviour in High-Volume GGBFS Concrete for Rigid Road Pavements. *ASCP*, **1**, 11 (2023).
38. Y. Ru, M. Gruninger, Y. Dou, Robust self-supervised symmetric nonnegative matrix factorization to the graph clustering. *Sci. Reports*, **15**, 7350 (2025).
39. Y. Huo, S. Gang, C. Guan, Fcihmrt: *Feature cross-layer interaction hybrid method based on Res2Net and transformer for remote sensing scene classification, Electronics*, **12**, 4362 (2023).
40. J. Singh, R. Abraham, Magnetic Catalyst CdFe2O4: Direct Conversion of Thiols into Antibacterial Sulfonamides. *Biol. Mol. Chem.,* **2**, 13 (2024).